A demogenetic agent based model for the evolution of traits and genome architecture under sexual selection

Louise Chevalier[1,*]

François de Coligny[2]

Jacques Labonne[1]

1. Universite de Pau et des Pays de l'Adour, E2S UPPA, INRAE, ECOBIOP, Saint-Pée-sur-Nivelle, France

2. AMAP, Univ Montpellier, CIRAD, CNRS, INRAE, IRD, 34000 Montpellier, France

∗ Corresponding author; e-mail: louise.chevalier@inrae.fr.

keyword: sexual selection, demogenetic agent-based model, mutual mate choice, competition, preference, pleiotropy, polygeny.

ABSTRACT

Sexual selection has long been known to favor the evolution of mating behaviors such as mate preference and competition, and to affect their genetic architecture, for instance by favoring genetic correlation between some traits. Reciprocally, genetic architecture can affect the expression and the evolvability of traits and mating behaviors. But sexual selection is highly context-dependent, making interactions between individuals a central process in evolution, governing the transmission of genotypes to the next generation. This loop between the genetic structure conditioning the expression and evolution of traits and behaviour, and the feedback of this phenotypic evolution on the architecture of the genome in the dynamic context of sexual selection, has yet to be thoroughly investigated. We argue that demogenetic agent-based models (DG-ABM) are especially suited to tackle such a challenge because they allow explicit modelling of both the genetic architecture of traits (polygyny, pleiotropy) and the behavioural interactions in a dynamic population context. We here present a DG-ABM able to simultaneously track individual variation in traits (such as gametic investment, preference, competitiveness), fitness and genetic architecture throughout evolution, accounting for the physical structure of the genome (genetic map). Using three simulation experiments, we compare various mating systems and show that behavioral interactions during mating triggered some complex retroactions in our model, between fitness, population demography, and genome architecture, placing interactions between individuals at the core of evolution through sexual selection. DG-ABMs can, therefore, relate to theoretical patterns expected at the population level from simpler analytical models in evolutionary biology, and at the same time provide a more comprehensive framework regarding individual trait and behaviour variation, that is usually envisioned separately from genome architecture in behavioural ecology.

INTRODUCTION

Sexual selection has long been recognized as an evolutionary force shaping mating behaviours and morphological traits in populations (Darwin, 1872; Fisher, 1915; Jones and Ratterman, 2009), and has been invoked as a driving force behind speciation (Lande, 1981; Ritchie, 2007). Evolutionary biology, therefore, predicts change in the genotypic and phenotypic composition of a population due to sexual selection (Lande, 1981; Lande and Arnold, 1985; Pomiankowski and Iwasa, 1998; Tazzyman and Iwasa, 2010). Such predictions, based on population genetics, quantitative genetics, or adaptive dynamics rely on simplifying assumptions concerning mating processes and do not explicitly represent the pairing dynamics during mating.

However, sexual selection is fundamentally a behavioural process and complex behavioural interactions between individuals are likely to affect evolution (Bailey and Moore, 2012; Kokko et al., 2015; Moore et al., 1997; Muniz and Machado, 2018; Wolf et al., 1999). This social part of the environment is indeed one of the most dynamic sources of variation an organism might experience during its lifetime (Kent et al., 2008; Krupp et al., 2008; West-Eberhard, 1983). To understand the effect of the variable social environment (e.g., the availability of partners of various qualities) and frequency-dependent strategies (i.e. the outcome of a tactic depends on the tactics of others) on the evolution of mating behaviours, models in behavioral ecology generally use game-theory approach (Ramsey, 2011; Smith, 1976). Alternatively, if models in evolutionary biology pay little attention to the interactions between individuals, they highlight the role of genetic architecture in determining the trajectory of evolutionary change and show that genetic variance and covariance have a potentially strong impact on evolution (Hansen, 2003; Iwasa and Pomiankowski, 1995; Iwasa et al., 1991; Lande, 1976, 1981; Matessi and Di Pasquale, 1996; Walsh and Blows, 2009). Yet, mathematical resolution often requires a simplified representation of genetic architecture. For instance, in quantitative genetics, the genetic architecture of traits is described in terms of genetic variance and covariance which are supposed constant (Falconer et al. 1996, e.g. Connallon 2015; Iwasa and Pomiankowski

1995; Iwasa et al. 1991; Lande 1976, 1981). A set of simplifying assumptions justify this approximation (additivity, linkage equilibrium, infinite population size, multivariate Gaussian distribution of allelic effects). However, in a more realistic view of the world, finite population size induces fluctuations in the genetic variance and covariance, as genetic drift induces a change in allelic frequencies (Jones et al., 2003, 2007; Roff and Mousseau, 1999; Shaw et al., 1995; Steppan et al., 2002). Furthermore, frequency-dependent selection can increase genetic variance by favoring rare variants that differ from the most common (Sasaki and Dieckmann, 2011), and correlational selection can increase genetic covariance by favoring genetic correlation between traits (Lande, 1980; Matuszewski et al., 2014). Importantly, such changes in genetic characteristics certainly result in changes in genetic architecture and may in turn impact evolution (Debarre and Otto, 2016; Jones et al., 2014; Wakano and Iwasa, 2013; Wakano and Lehmann, 2014).

To better characterize the role of sexual selection in shaping mating behaviours, genetic architecture, and demography of the population, we, therefore, need to address the following questions: How do social interactions during reproduction affect the architecture of the genome? How does the evolution of genetic architecture, in turn, impact the evolution of traits and consequently affect demographic characteristics of the population? And how does the physical structure of the genome (number of genes involved, mutation rate, linkage disequilibrium) constraint this evolution?

The current challenge is, therefore, to explicitly take into account the context-dependence effect of sexual selection (generated by mating dynamics) on the transmission of genotypes to the next generation and on the evolution of the genetic architecture. Demogenetic agent-based modeling (DG-ABM) is an interesting approach to tackle this challenge (DeAngelis and Mooij, 2005; Oddou-Muratorio and Davi, 2014; Piou and Prévost, 2012). It is well suited to explicitly represent complex behavioural interactions between individuals (mating systems for instance), while also representing genome structure and transmission mechanisms. The present paper describes such a model and its ability to simulate the evolutionary loop between traits (or mating behaviours) and genome. The model assumes a trade-off between survival and reproductive investment, each reproductive trait being determined

by a user-specified genetic map. Reproduction is the outcome of interactions between individuals, potentially including competition for mates, and preference. We propose three simulation experiments to illustrate the potential of such modelling approach.

In a first experiment, we simulate and track the complex evolutionary dynamics of a chosen case study: coevolution of gametic investment and preference under mutual mate choice. In a second experiment, we simulate the evolution of gametic investment under four different mating systems (absence or presence of preference and/or competition) and investigate to what extent the evolution of reproductive traits in each mating system affect the functional organization of the architecture of the genome in term of pleiotropy and polygeny. The third and last simulation experiment investigates the effects of the physical structure of the genome (maximum number of loci in the genome and linkage disequilibrium) on traits evolution, and how this, in turn, affect the evolution of genetic architecture in terms of pleiotropy and polygeny. We finish by discussing the potential for such models to further our understanding of evolution in an integrated framework, and their ability to relate microevolutionary mechanisms to macroevolutionary patterns.

METHODS

We here give an extensive description of the model in the spirit of the ODD protocol (Grimm et al., 2006). The model can be downloaded at `https://forgemia.inra.fr/louise.chevalier/runaway`

An overview of the demogenetic agent based model

Purpose: The purpose of the model is to investigate the co-evolution between reproductive traits under sexual selection and their genetic architecture, taking into account mating behaviour, genetic and demographic characteristics of the population.

State variables and scales: This individual-based model uses a discrete temporal scale and is not spatially explicit. The time horizon of the model is in the order of a thousand generations. Three levels are considered: the gene level, the individual level, and the population level. At the gene level, genes are characterized by their alleles, which code for various genetic values depending on the number of traits simulated. They are also characterized by their position in the genome and their recombination probabilities with other genes. Such a position is invariant during the simulation because we do not wish to simulate the physical evolution of the genome. Individuals are characterized by the following state variables: identity number, sex, age, lifetime reproductive success and the genetic values of three traits: the gametic investment G, the preference P and the competitiveness C. The population level is characterized by the following state variables: population size, allelic diversity, mean allelic values and standard deviations for the two traits on each gene, mean and standard deviation of traits values and mean lifetime reproductive success. Note that the population level can be subdivided during reproduction, to create smaller mating groups and mimic spatial or temporal isolation during the breeding season.

Process overview and scheduling: The process for simulation is described below and can be seen in Appendix A1. The model proceeds in generational time steps. Within each generation or time step, four procedures are processed in the following order: survival, mate choice, reproduction, genetic mutations. Within the survival procedure, the default probability of surviving for an individual depends on population size (density dependence) and on its reproductive effort (which is the sum of the genetic values for costly traits). Within the mate choice procedure, mating groups of a user-specified size are formed by drawing lots of individuals from the population, then individuals from the same mating group encounter each other (randomly or according to their values of competitiveness, sequential encounter, Gimelfarb 1988), and they choose to mate or not with the encountered partner. If individuals make up a couple they will become unavailable to mate again for the present time step. Within the reproduction procedure, each parent produces gametes and the offspring are created by the random fusion of the parent gametes, their sex is randomly assigned. Within the genetic mutation procedure, each allele might be substituted by a new one. New alleles are assumed to be created by mutation, and their genetic values for each trait are drawn in independent Beta distributions by default, whose shape parameters are defined at the initialization stage (paragraph *Initialization*). The user-defined mutation rate is assumed to be constant throughout the genome. Because survival (S) partly depends on reproductive effort, it can therefore also evolve, allowing individuals to potentially participate in more than one reproduction (i.e., iteroparity evolution).

Details

Survival: The probability of surviving to the next reproduction event is determined as follows:

$$S = \frac{1}{(1+R)(1+\frac{N}{K})} \tag{1}$$

where N is the population size, K an indicator of resource limitation in the environment (akin, but not equal, to carrying capacity), R the sum of the genetic values of costly traits of the individual. Eq. 1 states that individual survival results from the interaction between two components. The first component is demographic ($\frac{1}{1+N/K}$), this formula corresponds to the survival rate of the population in considering that survival is solely density-dependent. The second component is individual ($\frac{1}{1+R}$), this formula states that individual survival is maximum when energy invested into reproduction is null, and that S decreases when R increases. Intuitively, if $N/K = 1$ (close to a demographic equilibrium) and if $R = 1$, then both components affect the survival equally. If the population size drops below K but $R = 1$, then survival rate will increase, making R a relatively greater contributor to survival (see Fig. 1). As a consequence, the model can evolve towards semelparity (low survival, single reproduction) or iteroparity (higher survival leading to potential multiple reproductions).

Mating behaviour: During reproduction, the population is first divided into mating groups of user-specified size M. Population sex ratio is $1:1$ but the sex ratio within each group can vary, due to random sampling. Then, within each mating group, mating processes occur, individuals mating only once per time step. The model can represent different mating systems:

(1) random mating: pairs of individuals from the same mating group but with different sex are formed randomly. Once a pair is formed, mating will occur. Mated individuals are not available for further mating for the current time step. Note that if M is not a pair

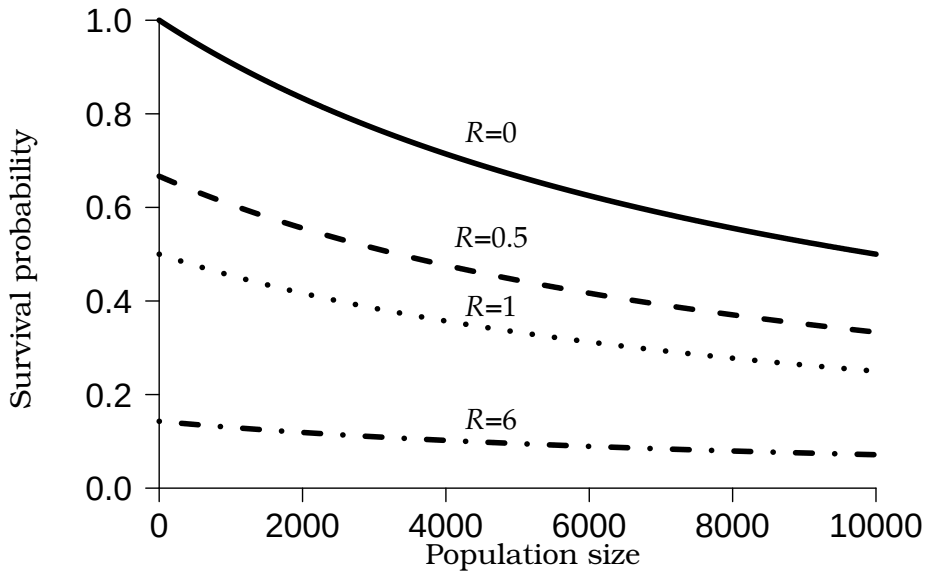

Figure 1: survival probability as a function of population size for different values of R. with resource limitation parameter K=10000.

number, or if all partners of one sex have mated, some individuals will remain unmated for the current time step.

(2) random encounter with preference: pairs of individuals from the same mating group but of the opposite sex are randomly drawn, but each individual chooses to accept the potential partner based on its preference trait. If both partners mutually accept each other, they become unavailable for further mating for the current time step. If at least one individual rejects the mating, both of them return in the mating group and yet again two individuals are randomly drawn from the mating group.

(3) competitive encounter without preference: Individuals from the same mating group but with opposite sex encounter each other based on their value of competitiveness C. For each pair of individuals thus formed, mating will occur. Mated individuals are not available for further mating for the current time step. When M is not a pair number, or

if one sex is no more available, the less competitive individuals of the mating group will remain unmated.

(4) competitive encounter with preference: Here again, individuals from the same mating group but with opposite sex encounter each other based on their value of competitiveness C. Within each pair thus formed, each individual chooses to accept the potential partner based on its own preference trait. If both partners mutually accept each other, they become unavailable for further mating for the current time step. If at least one individual rejects the mating, both of them return in the mating group and yet again two individuals are randomly drawn from the mating group.

Note that for each of these scenarios, the whole process is sequential: if a first pair is formed and both individuals mate, then the routine proceeds to the next pair. However, if the first pair is formed but mating does not occur, then it will affect the subsequent pair formation and potential related matings.

Preference model: The probability that an individual will accept the mating (Pm) is a function of his genetic value of Preference and his partner's Gametic investment (Eq.2).

$$Pm = \exp^{-\frac{(G_{pref}-G)^2}{2\nu^2}} \tag{2}$$

This equation indicates that individuals have a unimodal preference, i.e. they prefer a particular value of the gametic investment (G_{pref}) with a tolerance around this value (ν). The closer the gametic investment of the partner met is to the individual's preferred value, the higher the probability that the individual will accept the mating (Fig. 2). The parameter ν is set to 0.2 so that the integral of the preference function for an individual preferring a particular value of the gametic investment of 0.5 is equal to 0.5. Other forms of preference can also be simulated, such as monotonously increasing preference or threshold preference.

Competition model: Within a mating group of size M, the competitiveness C will be used to assess a non-random order of meeting between pairs of individuals. We assume

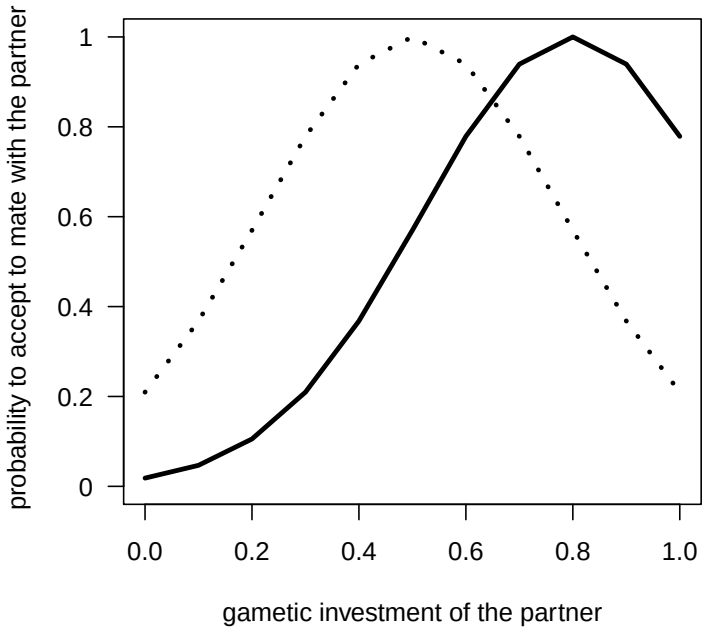

;

Figure 2: Probability that a potential partner will be accepted, as a function of the values of gametic investment of this partner for two different values of preference ($G_{pref} = 0.5$ dotted line, and $G_{pref} = 0.8$ plain line). Individuals differ in the value of G of their most preferred mate, but all individuals share the same tolerance ($\nu = 0.2$).

that the probability of meeting between two individuals is dependent on their respective competitiveness trait values. For instance, two individuals with high competitiveness values will probably meet first within the mating group. Then come pairs of individuals with contrasted competitiveness (one high, one low). Finally, two individuals with low competitiveness will meet at the end of the process, mostly. Pairs of individuals are thus ordered according to the product of their competitiveness. Note that if the meeting is not followed by a mating, each individual will be still available for mating. When individuals have mated once however, they are not available for further mating for the current time step and are removed from the list. Consequently, the less competitive individuals may miss reproduction if all opposite-sex partners in the mating group have already mated.

Reproduction: The gametes are composed of randomly chosen strands from each pair of homologous chromosomes. Recombination between successive genes may occur during the meiosis (depending on the values of recombination probabilities between genes). These probabilities are gathered in a table consisting of $n-1$ lines, n being the number of genes studied. Each line i contains a number between 0 and 0.5 which represents the probability of recombination between the ith gene and the $(i+1)^{th}$ gene. The number of offspring per couple is set to the average value of the parents' gametic investments multiplied by a demographic constant. The sex of the offspring is randomly attributed.

Genetic mutation: Right after fecundation, mutations might occur on the offspring genome. The rate of mutation is the probability each allele has to be substituted by a new one. Alleles mutation probability is user-defined, but the default value is set to 10^{-4} mutations per loci, which is within the range of spontaneous mutation rates estimated at particular genes in different organisms (Eyre-Walker and Keightley, 1999; Haldane, 1935; Muller, 1928).

Physical structure of the genome: All individuals share the same physical architecture of the genome, which is defined by the number of autosomes, the presence or absence of a sex chromosome, the number of genes, their location on the chromosomes and the probabilities of recombination between these genes. Each individual inherits two alleles for each gene (i.e. diploid). Alleles effects are described by continuous values and are additive within and between loci, i.e. dominance effects are not considered, such as the value of a trait corresponds to the sum of allelic values at every locus:

$$T_g = \sum_{l=1}^{l=n} (l_T^{a1} + l_T^{a2}) \tag{3}$$

with n the number of loci ($n = 100$), l_T^{a1} and l_T^{a2} values of the first and the second allele for the trait at the loci l. Individual phenotype is fully determined by the genotype, that is, environmental effects on phenotype are neglected, and heritability is thus assumed to be

unity. We define the landscape of allelic values for preference, gametic investment, and competitiveness by Beta distributions of user-specified shape parameters. Default values are [0.65, 24.5], resulting in a right-skewed distribution such as many alleles will have small values for the traits but still, some alleles will have relatively high values for the traits (Fig. 3A). As a consequence, under this set of parameters and using 10 loci, initial trait values for gametic investment followed the distribution showed in Fig. 3B with mean 0.5 and variance 0.02.

Genetic architecture: The genetic architecture is here defined as the distribution of allelic effects along the genome, and can, therefore, vary between individuals. According to universal pleiotropy assumption (Fisher, 1930; Hill and Zhang, 2012; Paaby and Rockman, 2013), each allele at each locus is specified by a vector of contribution to every trait. For instance in our case, in a two traits model with gametic investment and preference, each allele has two values, one for each trait. Alleles can, therefore, have a pleiotropic effect (if they have high values for both of the traits) or a modular effect (if the allelic value for one of the two traits is close to zero). Thus, an individual's genetic architecture can be pleiotropic if he carries alleles that have more similar effects for the different traits than they would have by chance, and conversely, an individual's genetic architecture can be modular if he carries alleles that have more different effects for the different traits than randomly expected.

Initialization: To initialize a simulation, three types of parameters are specified:

- demographic parameters: the resource limitation in the environment K and the initial population size.

- mating parameters: the mating system (e.g. random mating, random encounter with preference, competitive encounter without preference or competitive encounter with preference) and the size of the mating group M are also required. The minimal model is run using a single trait (G), more complex models can be run adding mating preference (P) and/or competitiveness (C).

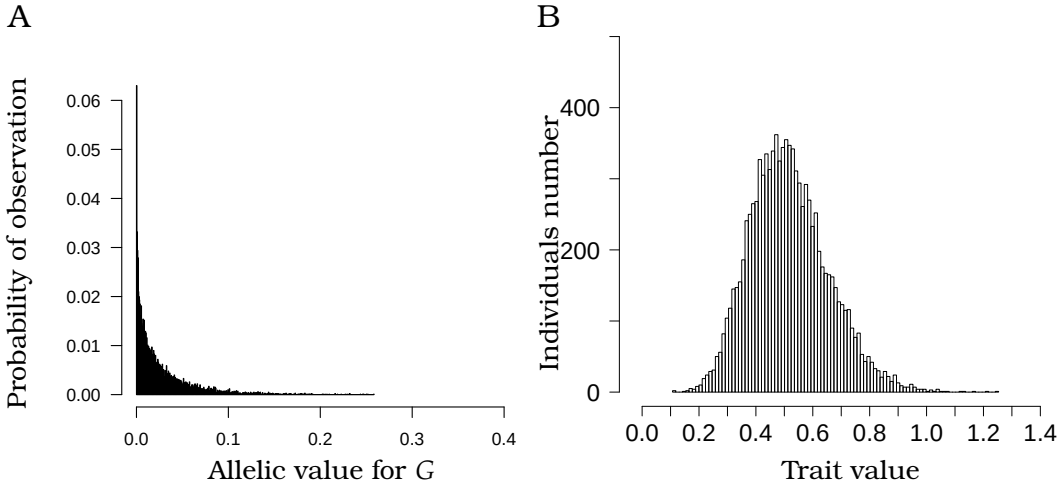

Figure 3: Example of allelic values distribution for the gametic investment (A) and consequent distribution of gametic investment trait values in the population (B). This distribution is obtained by drawing allelic values on the Beta distribution of shape parameters [0.65, 24.5].

- parameters for the physical structure of the genome: the number of chromosomes, the number of loci in the genome and their distribution on chromosomes. More specifically, the user specifies the probability of recombination between each contiguous pairs of loci, the maximum number of alleles per locus in the population, the allelic effects (i.e the values alleles can take), and the mutation rate.

Because initialization includes stochastic processes such as sampling in allelic effects distributions, initial states using the same parameters may vary. The model, however, allows starting several simulations out of a single initial state.

Design concept

We here describe the general concepts underlying the design of the model.

Fitness : Individuals do not seek to improve their fitness explicitly. Fitness improvement is obtained through genetic selection. Individual reproductive traits can indirectly improve individual fitness: high values of G enhance individuals reproductive success but have a survival cost, high values of P allow individuals to get a mate with high fecundity but have an *opportunity cost* (i.e. missing mating opportunities, De Jong and Sabelis 1991; Dechaume-Moncharmont et al. 2016; Fawcett et al. 2012), high values of C improve the mating success of individuals through priority access to mating partners, yet they do have a survival cost too.

Sensing, interactions, collectives : As previously described, during reproduction, the population is partitioned in several mating groups. Individuals sense and interact with potential sexual partners and competitors within the scale of the mating group. However, such information will not affect their decision (*i.e.* no adaptive behaviour ABM wise), only the outcome of interactions.

Adaptation : Individual fitness is mainly determined by its reproductive behaviour relative to other strategies. Indeed individual success during reproduction depends on opposite-sex preference and availability and same-sex competitiveness and preference. Individuals are therefore more or less adapted to their social environment. Individuals presenting preference for a very rare trait value in the population may not be socially adapted and entail the risk of not finding a mate, thereby compromising their fitness. Individuals also need to adapt to an extrinsic part of environment which is represented by habitat resources limitation. A typically non-adapted individual would present traits values that do not allow him to survive until reproduction in this environment.

Stochasticity : Because we use an agent-based model, most processes are inherently stochastic. Survival is, for instance, the realization of a Bernouilli random draw. Mating systems are also an important source of stochasticity. First, individuals are sampled randomly to constitute mating groups. Then, when they do not express competitiveness, individuals randomly encounter each other within each mating group. Mate choice itself is a highly stochastic process: it results from mutual acceptance of both partners, through their respective mating preference which is a probabilistic function, so to include an error of assessment of the mating partner quality. Lastly, the transmission of genetic information is also subject to stochasticity because we represent chromosome segregation and recombination during the meiosis and we also account for mutation risk.

Observation : The model can either be run in graphical user interface mode or script mode. In the former, the user can select if all time steps or only a subset should be memorized. In the memorized time steps, all objects (and therefore all individuals and their genomes) are observable. A wide panel of data extractors and visualizers is then available to analyze and illustrate the simulations. In script mode, only population-level variables are recorded over time.

For each simulation, we recorded different type of variables to characterize mechanisms of evolution: At the population level, trait evolution is monitored by measuring the average trait values in the population and its standard deviations, and the evolution rate of traits in Haldanes (Hendry and Kinnison 1999, Appendix A3); genetic architecture evolution is assessed by recording the distribution of allelic values at each locus on average in the population, which gives a statistical view of the genome at the population level. From this data we calculate two indicators to characterize genetic architecture:

(i) The degree of polygeny of the populational genome for a trait, that is the number of loci carrying alleles with an average value for a trait higher than would be expected if all loci contributed equally. The genetic value per loci is the average of the allelic values at this loci in the population at the current time step. This approach of polygeny measures the number of genes coding strongly for a trait relatively to the present distribution of

genetic values in the population.

(ii) The degree of pleiotropy of the populational genome for two traits indicates if genes have, in average, similar effects for both traits or if, on the contrary, genes have in average different effects for each of the traits. It is calculated from the sum of the squared difference between the mean allelic values for the two traits at every locus (Appendix A2). To obtain a pleiotropy index from this difference, it is necessary to be able to locate the value of this difference from the random values it could take (if the loci independently coded for both traits). For this purpose, a bootstrap is made. The pleiotropy index corresponds to the rank of the sum of the squared difference in the distribution of the sum of the squared differences calculated by bootstrap. The bootstrap is performed $n * (n - 1)$ times, with n the loci number. A ranking close to 0 means that the sum of differences in the average genetic values at each locus for the two traits is lower than expected by chance. A ranking close to the maximum index value means that the sum of differences in the average genetic values at each locus for the two traits is higher than expected by chance.

At the individual level: we record individuals lifetime reproductive success (fitness), individuals values of traits and individual level of pleiotropy between each couple of traits. The individual level of pleiotropy is calculated as the covariance between the allelic effects for the two traits.

SIMULATION EXPERIMENTS

Default parameters values used for all the simulations are the following: initial population size equal 10000, resource limitation is $K = 10000$, the size of the mating group M is set to the size of the population. The genetic map is, by default, made of 10 unlinked loci distributed over 10 chromosomes (i.e. recombination probability between adjacent locus is 0.5). The mutation rate is set to 10^{-4} mutations per loci.

Experiment 1: coevolution between preference and gametic investment

This first example introduces the evolutionary mechanics in the model, such as the relationships between demography, individual variation, and genetics, as well as the emergent patterns in the model. We here look at the evolution of gametic investment (G), under two different mating systems. First, with random mating, second, with preference (P) driven mating, wherein individuals select partners on their gametic investment. We track how the inclusion of a non-random mating system influences the evolution of G, and whether P itself co-evolves with the former trait. We examine both the dynamic phase of the evolution during the first generations and the later convergence phase around a pseudo-equilibrium after 5000 generations, in a single population.

Evolution of reproductive traits: Under random mating, G shows a substantial evolution from its initial value (of 0.5 average in the population) to reach a pseudo equilibrium around 0.7 after 200 generations (Fig.4 A). The standard deviation around this value remains stable throughout the simulation (around 0.1). The evolution rate of G calculated in Haldanes is accordingly moderately high during the first 200 generations and then stabilize to low values. During the early phase of the simulation, we observe a clear positive correlation between individual fitness and G, indicating that values above the mean for this trait are beneficial (i.e. directional selection). Once at the pseudo-equilibrium,

this relationship turns to a bell-shaped distribution, indicating stabilizing selection. Note that in this scenario, we also looked at the evolution of P as a non functional trait: this trait shows no evolution whatsoever, its average and standard deviation remaining stable throughout the simulation (Fig.4 A).

When mating is driven by P, the two traits increase quickly from their initial values (of 0.5 in average in the population) to reach maximum average values of 1.95 for G and 1.99 for P after about 200 generations (Fig.4 B). At this time, the standard deviation of the traits is maximal, around 0.2. Then the mean values of traits and their standard deviation decrease slowly overtime to reach mean values of 1.61 for G and 1.63 for P and standard deviations of 0.035 and 0.038 respectively. During the whole simulation, P is always greater than G, indicating that on average, the higher values of G are preferred in the population. The evolution rates of traits indicate a rapid evolution during the first 200 generations (with evolution rates that are in the upper range of values reported in the literature, Hendry and Kinnison, 1999), followed by a much slower evolution of traits. At the 100th generation, a snapshot of the fitness landscape shows that high values of G (of about 2) are advantageous (Fig.4 B). Later snapshots of the fitness landscapes confirm stabilizing selection, as well as an erosion of variance of G in the population with time (Fig.4 B). The emergence of a genetic correlation between G and P sheds some light on the rapid joint evolution of traits (Appendix B1). This correlation arises because individuals with high P choose individuals with high G, and thus, statistically, their offspring will inherit similar P and G values. It accentuates the joint evolution of the traits toward extreme values because P will then evolve under indirect selection (only because of the genetic correlation with G), while G is under increasing sexual selection (as P increases in the population) (e.g. Fisherian mechanism, Fisher 1915; Hall et al. 2000; Lande 1981). Interestingly, the positive correlation between the traits is transient as it reaches a maximum of 0.7 at time step 100, and then decreases to become negative (Appendix B1). Then, during the phase of stabilizing selection for the traits, the correlation oscillates around 0.

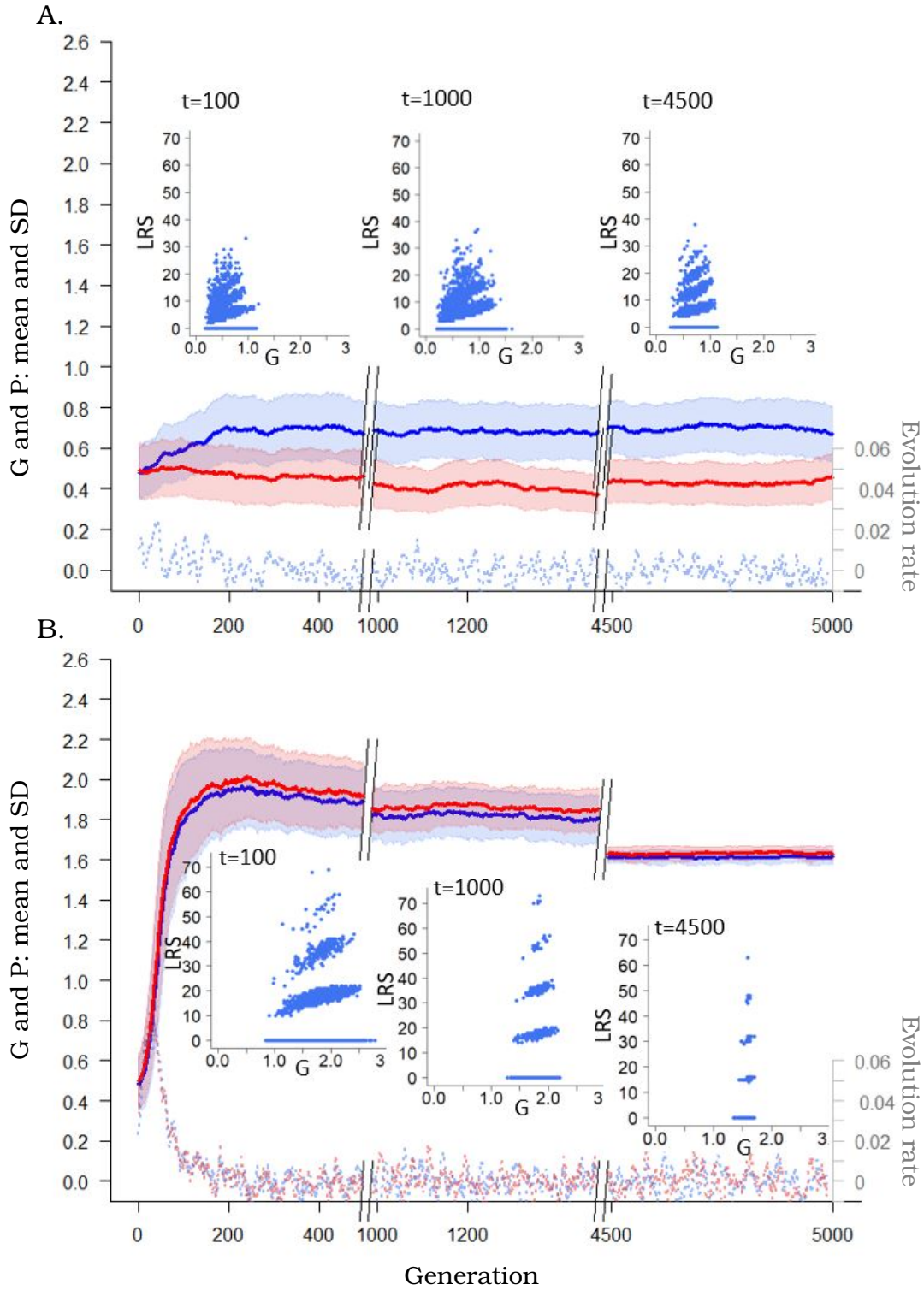

Figure 4: Evolution of G (in blue) and P (in red) in the population over 5000 time step, for one simulation of either (A) random mating , (B) preference driven mating. Mean values of traits are showed in thick lines and standard deviation values are represented in transparency. Also appear in the figure the evolution rates in Haldanes for the two traits (dashed lines) and the relationship between lifetime reproductive success (LRS) and G values at different time step during the simulation.

Genetic architecture evolution: A statistical view of the mean genome of the population shows the mean allelic value at each locus for the two traits (Fig. 5). Initially, due to the sampling of allelic values in random distributions, the mean allelic values are quasi uniformly distributed along the genome. At this moment, all loci have similar genetic values, with some loci having a mean value which is very slightly above average and others which are very slightly below average, leading to an average polygeny of about 5 for both traits. After 5000 generations, the allelic values are not evenly distributed over the genome, some genes coding much higher than the average for a trait (e.g. $l1$, $l7$, $l9$, $l10$ for G) whereas others code much lower than the average (e.g. $l4$, $l5$, $l6$, $l8$ for G), though that difference is not well reflected in the level of polygeny, which is still around 5 for both G and P. Remarkably, loci having a very high effect on one of the traits also have a very low effect on the other trait (e.g. $l4$, $l5$, $l7$, $l10$). Therefore it seems that the genetic architecture evolved toward modularity, with a differentiation of the genes coding for the trait G from the gene coding for the trait P. This observation is supported by the fact that the level of modularity of individuals' genome is positively correlated with their lifetime reproductive success (Appendix B3). We here predict an absence of pleiotropy in a situation where we may have intuitively expected pleiotropy to evolve. Indeed, we supposed that if a mutation that positively affects G also affects P in a similar direction due to pleiotropy, then these new mutations will be transmitted and become fixed in the population due to the increased fitness of their bearers. But our results showed that alleles with low pleiotropic effects are fixed during directional selection so that modular genetic architecture emerges from evolution. This result is robust to other mutational landscapes (uniform law, Appendix B2) but could be challenged if environmental parameters were changed (K, M). Modular genetic architecture may confer an adaptive advantage by allowing the traits to vary independently and thus be optimized separately without interference, thus promoting adaptive evolution (Griswold, 2006; Hansen, 2003; Otto, 2004).

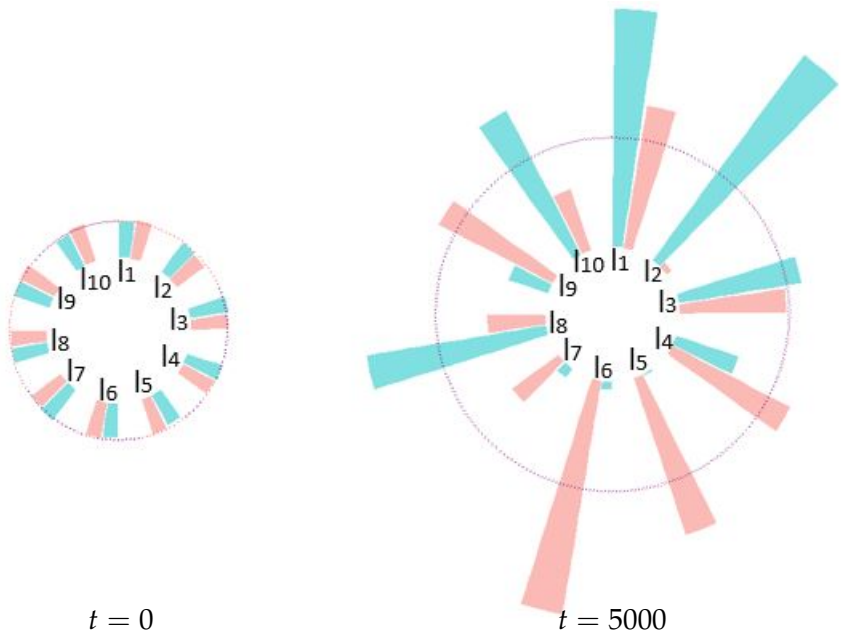

Figure 5: The mean genome in the population, at initialization (t=0) and after evolution over 5000 generation. The height of bars at each locus represents the mean value of alleles for this locus in the population for the gametic investment (bar in blue) and preference (bar in red). The dashed line indicates the average allelic value that each loci would have if all loci contributed equally to the value of the trait.

Experiment 2: Effect of mating systems on traits and genetic architecture evolution

In this experiment, we generalize the above approach to 4 different mating systems, named according to the number of traits expressed in each one (random mating G, random encounter and preference $G+P$, competitive encounter without preference $G+C$, competitive encounter with preference $G+C+P$, each time with 30 replications simulated over 5000 generations). We look at the effects of mating systems on traits evolution, but also at their rippling consequences on polygeny and pleiotropy in the genome.

Evolution of the reproductive traits: G evolves toward different values depending on the scenario, which is accompanied by different population sizes at the pseudo-equilibrium

(Fig. 6). When individuals express their preference (scenarios $R + P$ and $C + P$), P is favored by sexual selection, which promotes the evolution of G toward much higher values than in the random mating system, in which P evolves under genetic drift. As G is costly in terms of survival, its increase in the population leads to lower average survival, which translates into a lower pseudo-equilibrium population size (Fig. 6 B).

As previously explained, the joint evolution of P and G toward extreme values is caused by the build-up of correlation between the traits (Appendix B1), which is at the core of the mechanism of Runaway selection proposed by Fisher (1915).

Competitiveness (C) evolution is also conditioned by the simulation scenario. C is selected for (despite the associated survival cost) only when individuals also express their preference P on gametic investment G (scenario $G + P + C$), because in that case, the most competitive individuals are more likely to find a suitable mate. In the scenario without preference (scenario $G + C$), C is counter selected, its cost is too great when traded off against the possible benefit of reducing opportunity costs (e.g. the risk of not finding a mate). Indeed, in the present simulations, mating group size is equal to the population size, and opportunity cost under random mating is therefore negligible.

Whereas all simulations converge to the same value of G at the pseudo equilibrium under random mating, as soon as there is some preference or some competitive encounter, inter-simulations variance increases. It therefore underlines the importance of the complexity of behavioural interactions on the outcome of evolution.

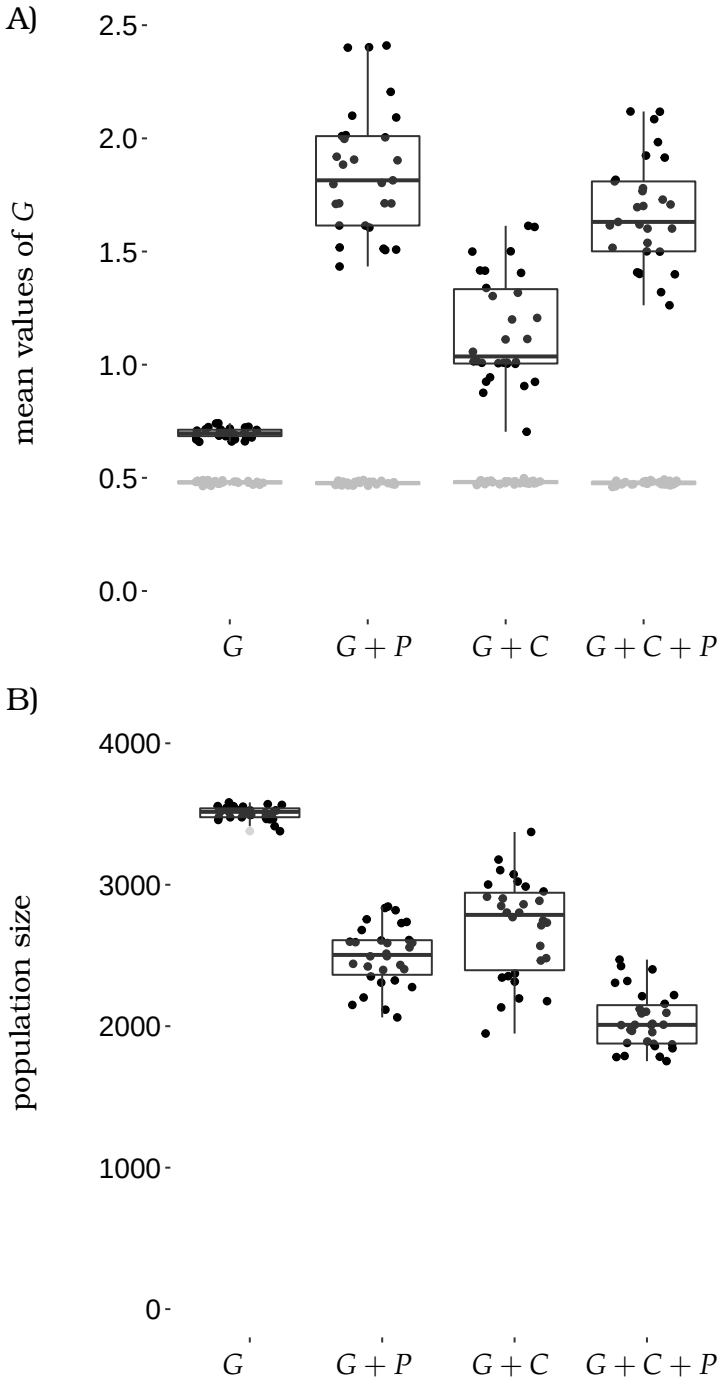

Figure 6: mean values of the gametic investment (A) and population size (B) , after evolution over 5000 time step. Each black dot represents a replication of the simulation. For gametic investment, initial values are displayed in grey. A boxplot indicates the 2.5, 25, 50, 75 and 97.5 quantiles of the distribution among replications. Four mating systems are simulated : random mating, noted G, random encounter and preference, noted $G+P$), competitive encounter without preference, noted $G+C$, competitive encounter and preference, noted $G+C+P$).

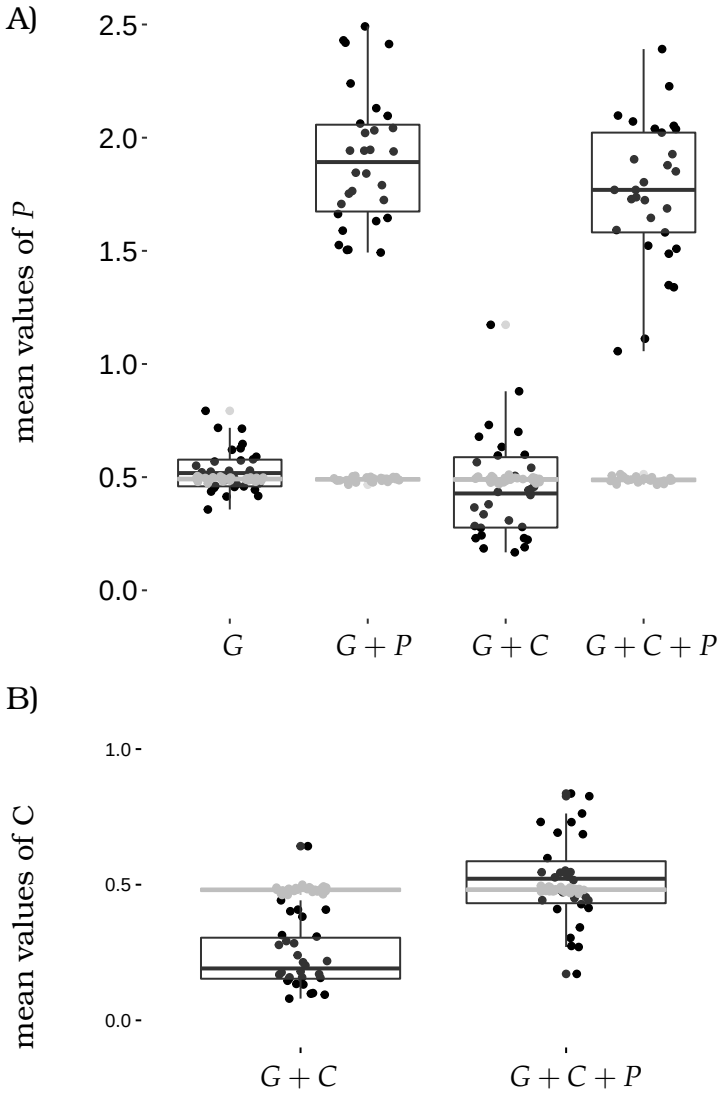

Figure 7: mean values of the preference (A) and competitiveness (B) , after evolution over 5000 time step. Each black dot represents a replication of the simulation. Initial values are displayed in grey. A boxplot indicates the 2.5, 25, 50, 75 and 97.5 quantiles of the distribution among replications. Four mating systems are simulated : random mating, noted G, random encounter and preference, noted $G+P$), competitive encounter without preference, noted $G+C$, competitive encounter and preference, noted $G+C+P$). For competitiveness only the two mating systems where the trait is involved are represented.

Genetic architecture evolution: Whatever the mating system investigated, and for the three reproductive traits, the degree of polygeny (i.e. the number of loci with an above-average effect) generally decreases from a mean number of about 5 to a mean number of about 4. This indicates that the relative contribution of loci to the total genetic value of each trait has somehow evolved, with some loci presenting a stronger relative contribution than in the initial situation.

Yet, the degree of pleiotropy evolves differently depending on the mating system Fig. 8. When individuals mate randomly, pleiotropy evolves randomly and there is no effect of initial pleiotropy: in simulations where the genome is initially pleiotropic by chance, the genome can evolve toward relatively high modularity, not illustrated here. However, when preference matters, the genome evolves towards increased modularity between G and P. This is also true in the presence of competition (scenario $G+P+C$), yet to a lesser extent. Remarkably, such increased evolution of modularity occurs in scenarios where there is co-evolution between the G and P (scenarios $G+P$ and $G+P+C$, Fig. 8.). Finally, there is no particular pattern of pleiotropy between G and C and between P and C (whatever the scenario, data not shown). We, therefore, observe that the number of traits considered, which also determines mating systems, mediates the evolution of the genome.

Within the scope of this paper, we did not change the mutation rate μ , the carrying capacity K and the mating group size M. Within these settings, preference reached high values whereas competitiveness barely evolved. We suspect that it would be a whole different matter if we had modified M. Indeed, in situations where individuals only meet a subset of the population to find their mate ($M <$ population size) the risk of not reproducing can be high, and consequently competition is expected to be stronger. In that case, traits may evolve differently; for instance, iteroparity (i.e low G, low P) can be favored as a form of "Bet Hedging" in time (Wilbur and Rudolf, 2006) and high competitiveness could be an advantage. This may, in turn, affect the evolution of genetic architecture.

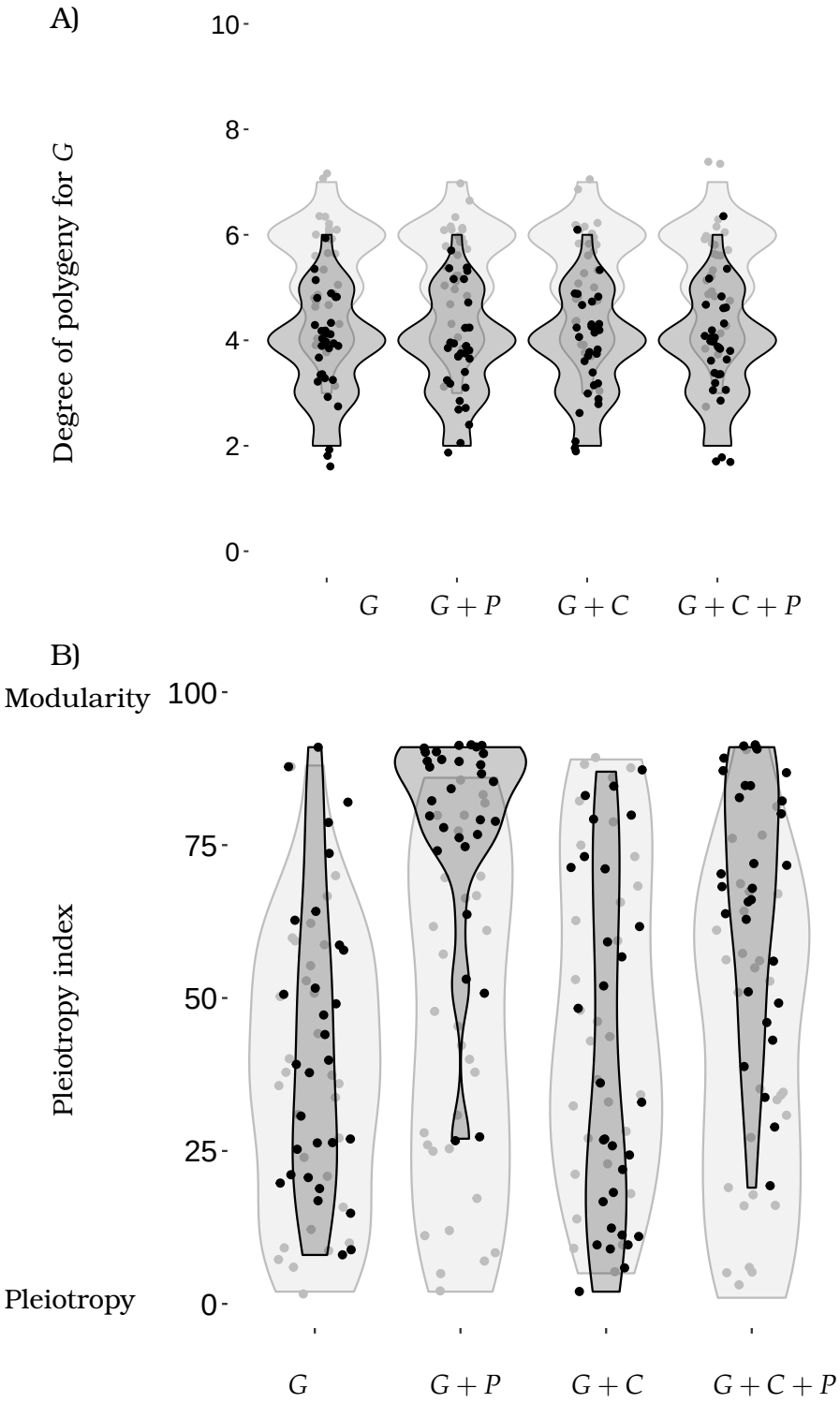

Figure 8: Degree of polygeny for G (A) and pleiotropy index between G and P (B) of the mean genome of the population. The measures are showed initially (in grey) and after evolution over 5000 time step (in black) for 30 replications for each mating system (random mating, random encounter and preference, competitive encounter without preference, competitive encounter and preference). Greyed areas indicate density probability for the distribution of points in the variation range.

Experiment 3: Effect of the physical structure of the genome on the co-evolution between gametic investment and preference

In this experiment, we extend Experiment 1 to three different physical structures of the genome. This is done by changing the genetic map describing the location and the maximum number of coding loci in the genome.

The first genetic map corresponds to the default settings, used in Experiments 1 and 2: 10 loci are represented and the probabilities of recombination between genes on each locus equal 0.5, meaning that all loci are independently segregated during the meiosis. This map corresponds to a case without physical linkage, where the genome is made of 10 chromosome pairs each carrying a single locus (potentially coding for both the traits G and P). In the second genetic map, 10 genes are distributed on 2 chromosomes (5 per chromosome). The probability of recombination between genes remains 0.5 between chromosomes but goes down to 0.01 within chromosomes, assuming close proximity of genes. This genetic map aims at simulating the effect of physical linkage between loci on the evolution of traits and genetic architecture. In the third genetic map, 100 unlinked loci are represented and the probabilities of recombination between genes on each loci are of 0.5. This map corresponds to a situation where the genome is made of 100 chromosome pairs each carrying a single locus. Compared to the previous genetic map, we thus authorize an increased maximum number of coding loci, and therefore more complex arrangements of the genetic architecture.

In order to get the same initial distribution of traits for all genetic maps, alleles values are drawn in different Beta distributions depending on the number of loci in the genome. Alleles values are drawn in a Beta distribution of shape parameters $[0.65, 24.5]$ when the genome is composed of 10 loci (Fig. 3) and of shape parameters $[0.06, 25]$ when the genome is composed of 100 loci (Appendix B4).

The evolution of reproductive traits: Under random mating, there is no effect of the genetic map on the evolution of G (dark grey values, Fig.9). When preference drives mating, the joint evolution between G and P is affected by the different genetic maps. Compared to Experiment 1 (10 unlinked loci), the inclusion of physical linkage (10 loci, 2 chromosomes) tends to slightly limit the coevolution between the traits. This result is surprising because one should expect that genetic linkage would favor the build-up of genetic correlation between traits and therefore would increase the joint evolution of traits. But on the contrary, here genetic linkage limits the rising of genetic correlation between the traits during the 100 first generations (Fig.10). Less surprisingly, genetic linkage also prevents the evolution of a negative correlation between traits such as that observed in scenario 10 unlinked loci (Fig.10).

When the genome is composed of 100 unlinked loci, the coevolution between traits is boosted towards much higher values (Fig.9). This is so because the genetic correlation between traits reaches higher values and is maintained over a much longer period (Fig.10).

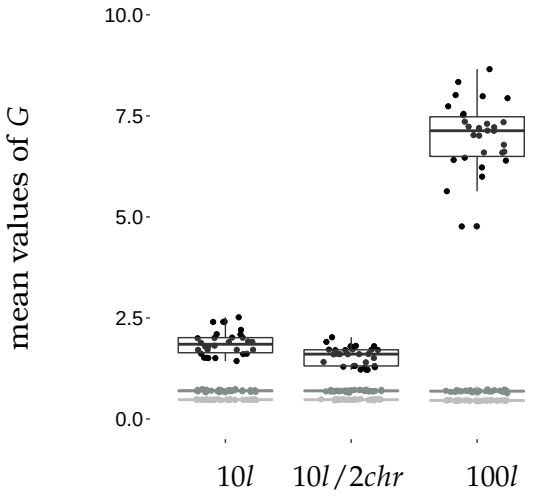

Figure 9: mean values of the gametic investment after evolution over 5000 time step. Each black dot represents a replication of the simulation. Initial values are displayed in light grey. Dark grey indicates the random mating system, black indicate preference driven mating system. 30 replications are performed for each mating system and for the three genetic maps. A boxplot indicates the 2.5, 25, 50, 75 and 97.5 quantiles of the distribution among replications.

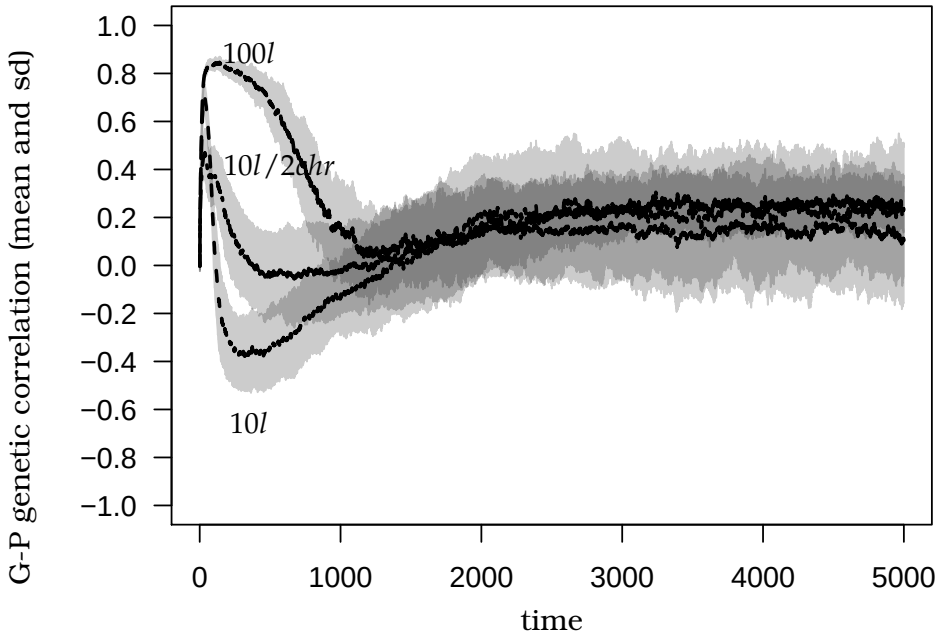

Figure 10: mean genetic correlations over 5000 generations (black line, and standard deviation around the mean, grey area) for 30 replications of the three genetic maps (10 loci on 10 chromosomes, 10 loci on 2 chromosomes and 100 loci on 100 chromosomes).

Genetic architecture evolution: The degree of polygeny for the gametic investment is not influenced by the level of genetic linkage when the genome is made of 10 unlinked loci (Appendix B5). When the genome is made of 100 unlinked loci, the degree of polygeny is higher; but reduced to the size of the genome, this represents about the same proportion as when the genome is made of 10 loci. Polygeny evolution, therefore, does not seem to be affected by the genome physical structure in our experiment. The level of pleiotropy, however, is affected by the genetic map. When considering 10 unlinked loci, pleiotropy seems counter-selected (as previously observed in the single replication of Experiment 1), whereas when these loci are linked, any level of pleiotropy can evolve. The linkage implies that neighbouring alleles will be transmitted together with a high probability, thereby offsetting the fitness benefit of modularity observed in Experiment 1. When the genome is composed of 100 unlinked loci, the genetic architecture evolves even more

strongly toward modularity.

Regardless of the size of the genome, all the genes are not recruited to code for each trait and the genome is divided between genes that strongly code for P and those that strongly code for G. Furthermore, a high number of locus increases the drive for modularity because more genes are available to distribute genetic effects.

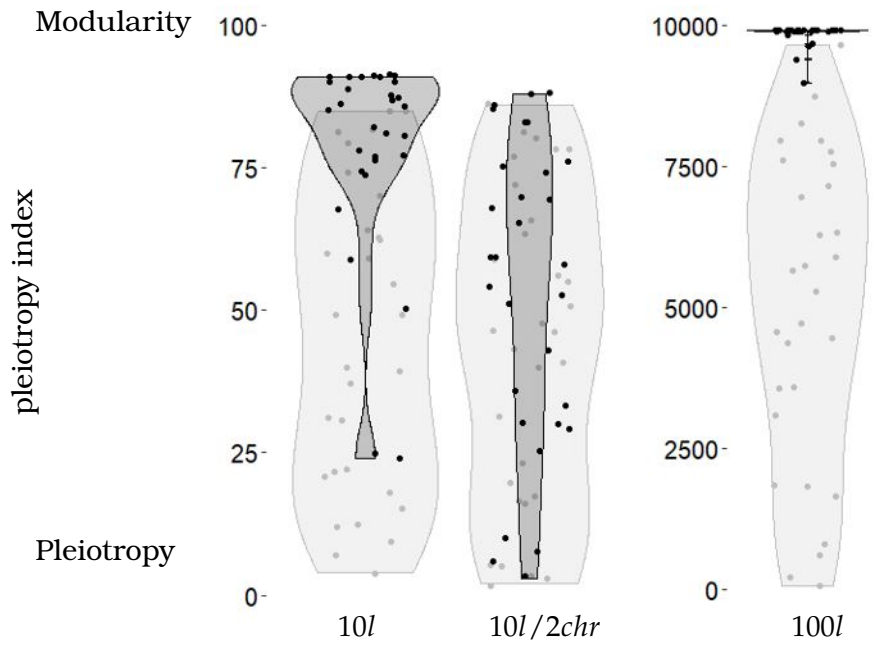

Figure 11: Pleiotropy index between the gametic investment and the preference. The measures are showed initially (in grey) and after evolution over 5000 time step (in black) for 30 replications for each genetic map (10 loci on 10 chromosomes, 10 loci on 2 chromosomes and 100 loci on 100 chromosomes). Greyed areas indicate density probability for the distribution of points in the variation range.

DISCUSSION

By capturing the processes linking genes, genome, individuals, groups, population, and environment levels, DG-ABMs offer new opportunities to study evolutionary dynamics in an integrative approach. One of the benefits of such an approach is that model predictions can, therefore, be analyzed at each of these levels, allowing comparisons with available empirical data and knowledge from a broad range of disciplines, in a single framework, instead of focusing only on one or two of these levels (Rittschof and Robinson, 2014). Another benefit of DG-ABMs is that they do not need to assume an equilibrium of genetic variance within populations (for instance, in terms of mutation and drift): on the contrary, they can focus on the dynamics of genetic variation, simultaneously at the population level and in terms of architecture. Likewise, they do not need to assume demographic equilibrium in terms of population growth rate or stable age distribution. DG-ABMs can, therefore, be applied to a large variety of issues in different - stable or dynamic- contexts, and can be used as a link between more theoretical approaches and empirical observations that rarely meet theoretical requirements. In the present study, using this approach, we have demonstrated that the interplay between genetics, demography, and behaviors is pivotal in predicting the evolution of traits and genetic architecture under sexual selection, whereas too often these disciplines are treated separately (Bengston et al., 2018; Rittschof and Robinson, 2014; Wilkinson et al., 2015). Most of our simulation experiments revolved around comparing various mating systems to a generally assumed random mating process. It appeared that departing from random mating triggered several complex retroactions in our model - between fitness, population demographic and genetic structure, and genome architecture - placing interactions between individuals at the core of evolution through sexual selection (Kokko et al., 2015; Muniz and Machado, 2018; Otto et al., 2008).

In the presented approach, wherein we kept control parameters constant along the simulations (K, μ, M, physical structure of the genome), two distinct evolutionary phases can be distinguished.

The first phase is the route toward a pseudo equilibrium and depends on initial conditions (values of traits, based on initial genetic architecture). The direction and speed of this route are of major interest: traits evolve through optimization of fitness through selection, although we do not specify the evolutionary optimum or the adaptive landscape *per se*, contrary to most models which assume a known evolutionary optimum (e.g; Guillaume and Otto 2012; Jones et al. 2003, 2014; Lande and Arnold 1985; Lorch et al. 2003; Matuszewski et al. 2014; Mead and Arnold 2004). We measure the variance of fitness throughout evolution, and we can, therefore, better understand the mechanisms that lead to the selection of some trait combinations and some particular genetic architectures. In this way, the model can also be used to assess the robustness of some previous and more simple theoretical models, in a more realistic framework. For instance, we can measure the correlation between traits, relate it to fitness at each generation, and simultaneously observe whether these correlations between traits foster – or not - the building of actual non-random allelic structure within the genome (here pleiotropy for instance). It allows us to show, among other things, that the building of genetic correlation between mating preferences and a trait - assumed by quantitative genetics approaches and at the core of Runaway selection (Fisher, 1915; Lande, 1981) - also occurs in our more complex model and explicitly arises from assortative mating process. But in our model, assortative mating is not assumed: it emerges from the evolution of preference and competitiveness, and interactions between individuals during the breeding season, achieving variable mating and reproductive success. Additionally, in the presented simulations, such genetic correlation was not accompanied by an increase of pleiotropy, whereas it was sometimes mentioned that pleiotropy could indeed foster such dynamics.

In addition, the role of environmental parameters on this dynamic phase is paramount, and we allow to simultaneously test for the effect of habitat resource (K), social parameter (M), and genetic constraints (mutation rate μ as well as the physical structure of the genome). All of these parameters will likely affect the genetic variance, which will in turn condition the speed of evolution. The study of these effects is central to the understanding of biodiversity dynamics and resilience, and our model could be used to investigate

variable mutation rates in time or along the genome, or to explore the effect of fluctuating resource in the environment or factors affecting the distribution of potential mating partners.

The second phase is characterized by having reached an evolutionary pseudo equilibrium, the mean and variance of traits being stable within a population. Likewise, K, mutation rate, the physical structure of the genome and mating group size may have a strong impact on the outcome of the simulations. First, it can affect what are the mean values for traits, population size, and genetic architecture, but also their respective variances at equilibrium. Although these equilibria can seldom be observed in nature, where many environmental parameters fluctuate, they can nevertheless be used as a reference point to compare (qualitatively) our predictions with theoretical models. For instance, our results on genetic architecture suggest that pleiotropy can be counter selected in some situations even in the absence of functional trade-off in gene activities (Guillaume and Otto, 2012), and support the idea that selection pressures may substantially shape the distribution of pleiotropic effects among genes (Cheverud, 1996; Hansen, 2003; Pigliucci, 2008).

Additionally, predictions at equilibrium are of particular interest when we consider to what extent different replications for the same scenario may converge. The difference between replications can be seen as a proxy of variance between populations, indicating that despite having the same initial conditions, environment, and constraints, two populations may diverge to some extent (when not related by dispersal, in the current model). This is of major interest for empiricists trying to investigate parallel evolution of populations experimenting similar environments (Bolnick et al., 2018; Oke et al., 2017; Schwartz and Hendry, 2007); in some cases, one should not be surprised to find substantially variable evolutionary outputs. In the core of our model, it is noteworthy to underline that such divergences mainly occur due to interactions between individuals (such as mate choice), and are therefore highly sensitive to stochastic processes. We suggest that such a mechanism could also play a major role in natural populations, stressing the importance to study and understand behavioural interactions in relation to the environment.

Arguably, the presented results for each of the three simulation experiments only envision a small span of the possible variation in mating behaviours, the physical structure of the genome or environmental control. In its present shape, our model already includes alternative scenarios to explore, that is of great interest to evolutionary and behavioural ecologists. For instance, the shape and modalities of the preference function can be easily modified by users to address fixed or probabilistic threshold responses. By modifying the physical structure of the genome, we can simulate sexual chromosomes, thereby authorizing sexual differentiation in traits genetic values. Such differences may, in turn, affect survival differently between sexes, which would, therefore, affect the operational sex ratio within mating groups, possibly modifying the strength of sexual selection, and retroactively participating in the divergent evolution of the genome between males and females (Bonduriansky and Chenoweth, 2009; Chapman et al., 2003; Gibson et al., 2002; Hammer et al., 2008). This example indicates how all levels are naturally entangled in the individual based demogenetic approach. Notably, we have not yet included explicitly the role of parental care as well as the question of gamete size, two questions that can be central in the evolution of mating systems (Fromhage and Jennions, 2016; Kokko and Jennions, 2008; Lehtonen et al., 2012, 2016; Parker et al., 1972). For now, parental care is implicitly assumed, since the calculation of fecundity (as the mean of both partners gametic investments) somehow implies that both parents contribute to reproductive success.

CONCLUSION

Beyond the question of co-evolution between gametic investment and preference, the DG-ABM modelling approach allows to make much more comprehensive predictions on biological systems: for instance, instead of focusing on the evolutionary equilibria of phenotypic trait values, we here provide a complete picture of what such equilibria entail also in term of genetic architecture and demography. Namely, for such dynamics to occur, we demonstrate that demographic characteristics will also reach non-random values (level of iteroparity and survival, opportunity cost, population size) and that this

may come with the building of non-random allelic structure within the genome (level of pleiotropy and polygeny). Such projection also allows capturing more efficiently the evolutionary constraints that will control the outcome of adaptive evolution (genetic architecture, phenotypic correlation, demographic processes). We hope that this model can motivate further work on the link between the physical structure of the genome and variations in mating systems or life histories (e.g Charlesworth and Wright 2001; Lamichhaney et al. 2016; Misevic et al. 2006; Plomion et al. 2018; Sinervo and Svensson 2002).

ACKNOWLEDGEMENTS

The present model was coded on the CAPSIS-4 modelling platform (http://capsis.cirad.fr, Dufour-Kowalski et al. 2012) maintained by F. de Coligny and N. Beudez, who also helped in developing parts of the code. We also thank A. Courtiol for thoughtful suggestions on an earlier version of the model.

Appendix A: supplementary methods

A1. The model

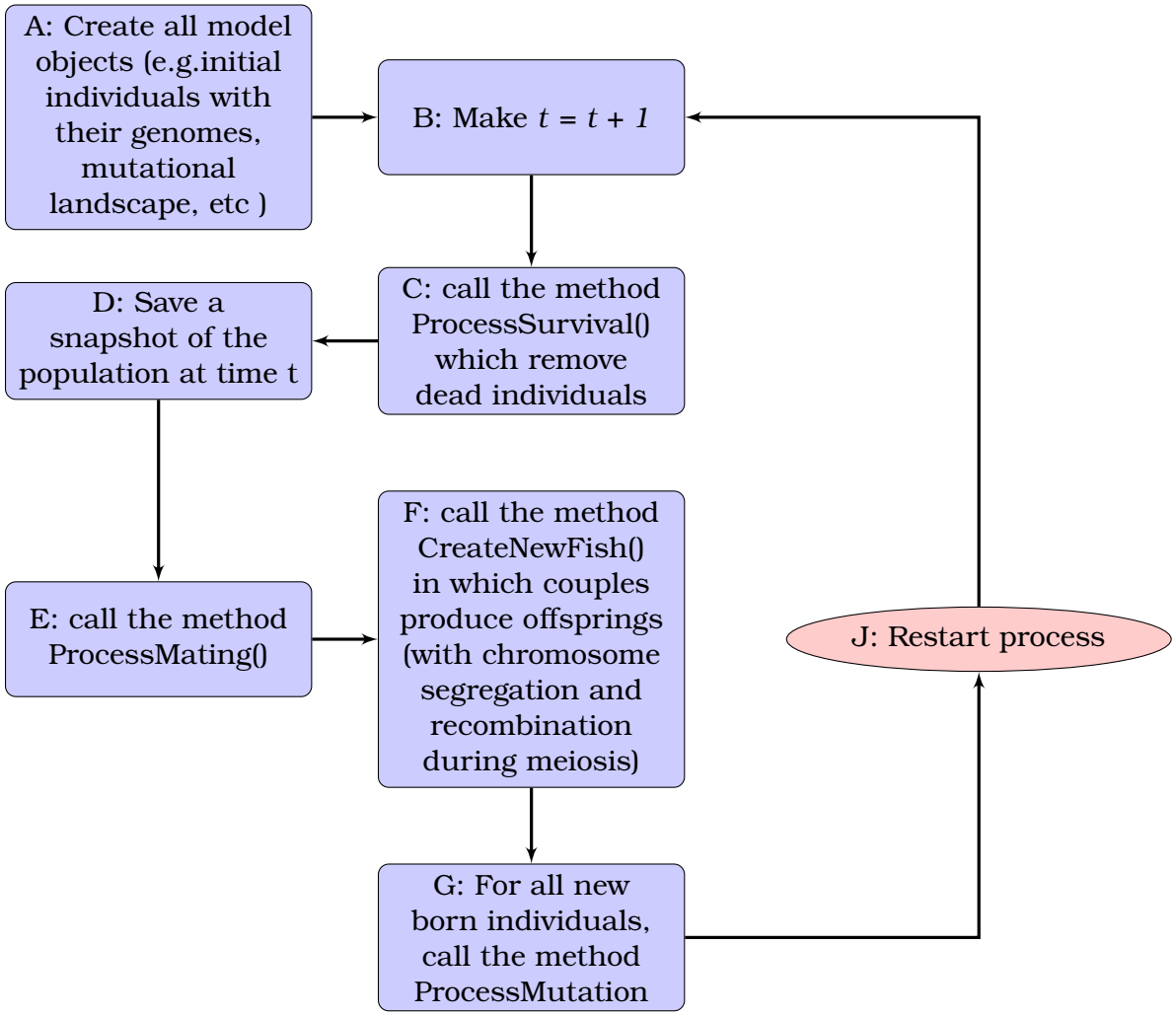

Figure A1: Flowchart showing the order of the processes implemented in the model.

A2. calculation of the pleiotropy index

$$SSD = \sum_{n=l_0}^{n=l_x} [(G_n - P_n)^2] \tag{A2}$$

with G_n and P_n the mean allelic values at loci n for G and P and x the number of loci. SSD is the sum of square differences between allelic values for the traits at every loci. The pleiotropy index corresponds to the rank of the sum of the squared difference in the distribution of the sum of the squared differences calculated by bootstrap.

A3. Evolutionary rate in Haldanes

We measure evolutionary rate in Haldanes using the same formula as Hendry and Kinninson (1999):

$$h = \frac{\frac{x_2}{s_p} - \frac{x1}{s_p}}{g} \tag{A3}$$

where x_2 and x_1 represent mean trait values for the single population at two different times, s_p is the pooled standard deviation $s_p = \frac{(n1-1)*(sd_{log(x1)})^2+(n2-1)*(sd_{log(x2)})^2)}{(n1-1)+(n2-1))}$, and g is the number of generations separating the two different times.

Appendix B: supplementary figures

B1. Genetic correlation between G and P

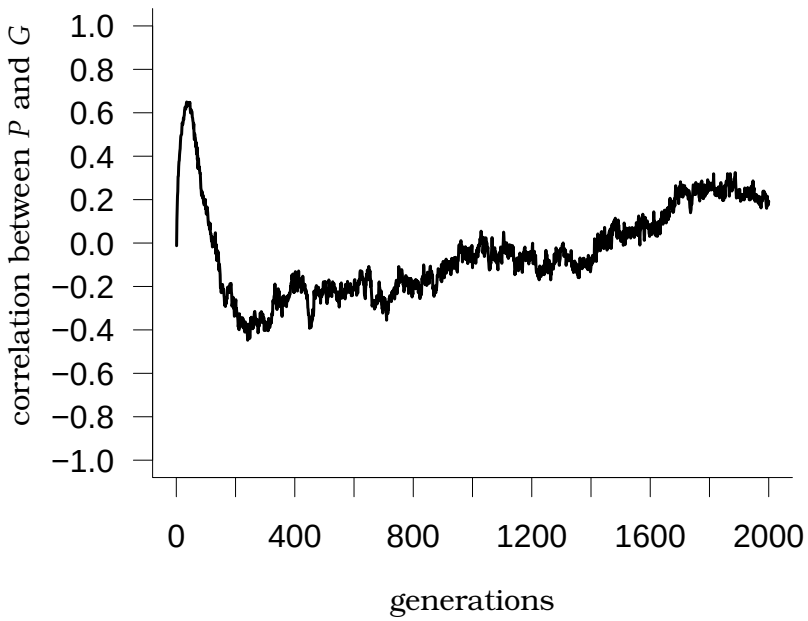

Figure B1: Correlation between individual preference values and individual gametic investment values in the population, for one simulation of the mating system ($G + P$).

B2.Pleiotropy index with a uniform mutational landscape

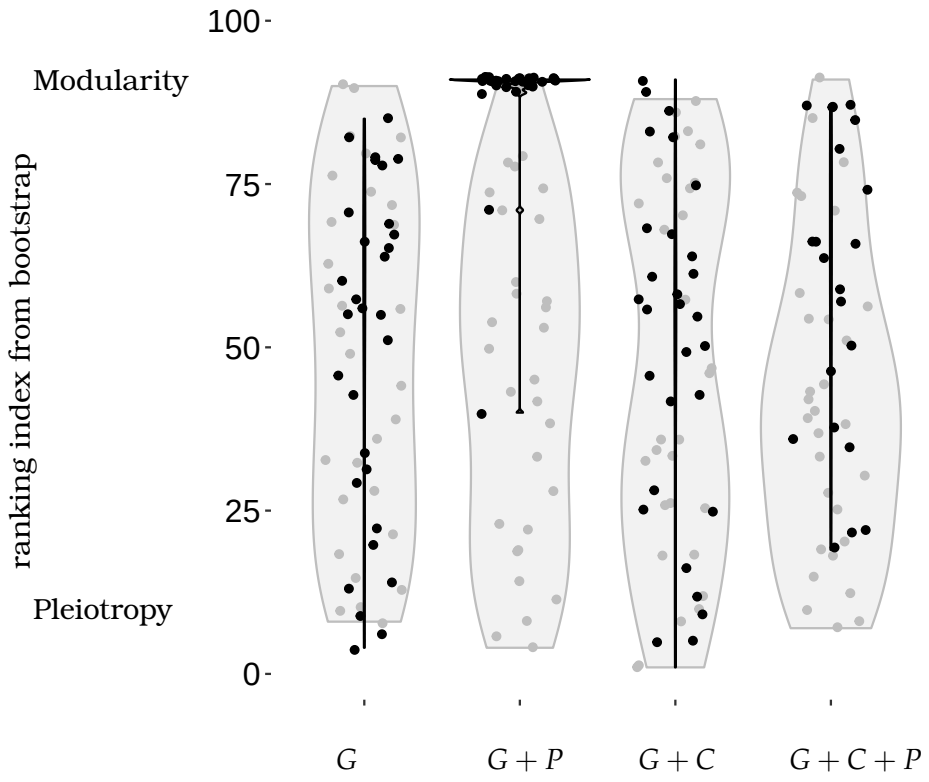

Figure B2: Pleiotropy index between G and P of the mean genome in the population. The measures are showed initially (in grey) and after evolution over 5000 time step (in black) for 30 replications for each mating system (random encounter without preference, random encounter and preference, competitive encounter without preference, competitive encounter and preference). Greyed areas indicate density probability for the distribution of points in the variation range. The mutational landscape follows an uniform distribution.

B3. Lifetime reproductive success as a function of individual pleiotropy index

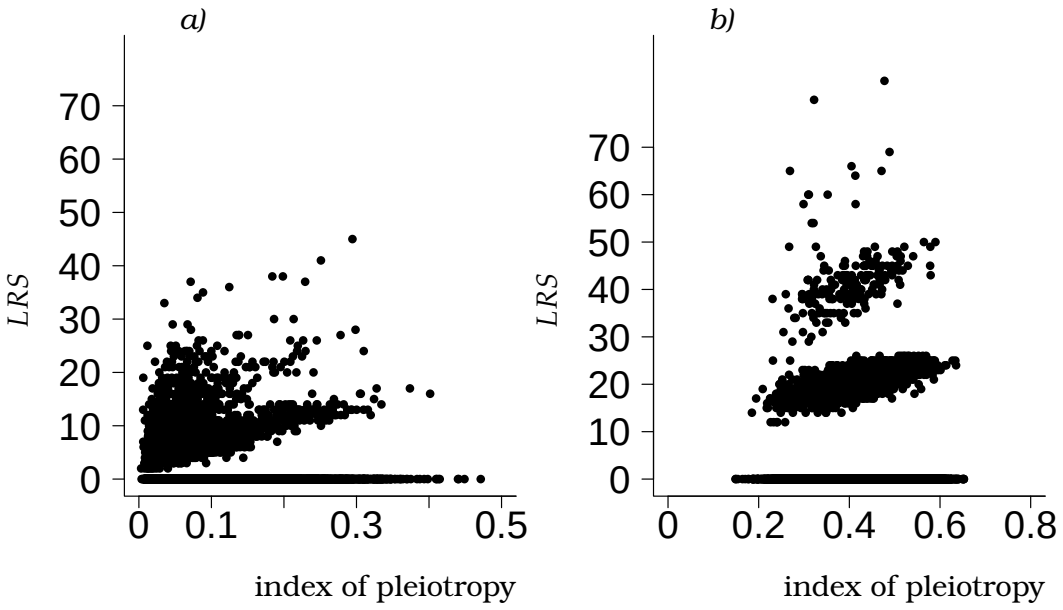

Figure B3: The lifetime reproductive success of individuals as a function of the index of pleiotropy of their genome at the 100th (a) and 1000th (b) time steps. The index of pleiotropy is the sum of the squared distances between the mean genetic values for G and P at each locus. Mating system: $G + P$

B4. Distribution of allelic values when the genetic map is made of 100 loci

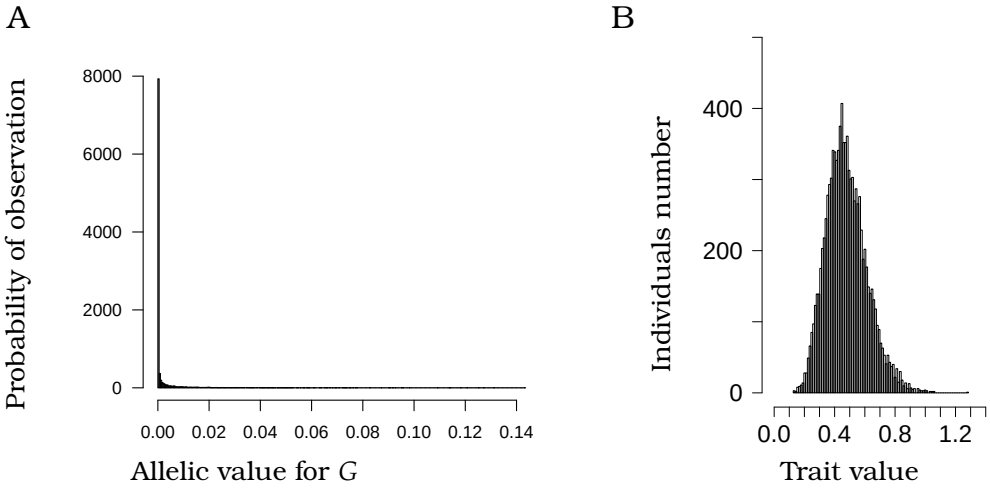

Figure B4: When the genetic map has 100 loci, allelic values for the gametic investment follow a distribution Beta[0.065, 24.5] (A) , and consequent distribution of gametic investment trait values in the population (B).

B5. Effect of the genetic map on the degree of polygeny

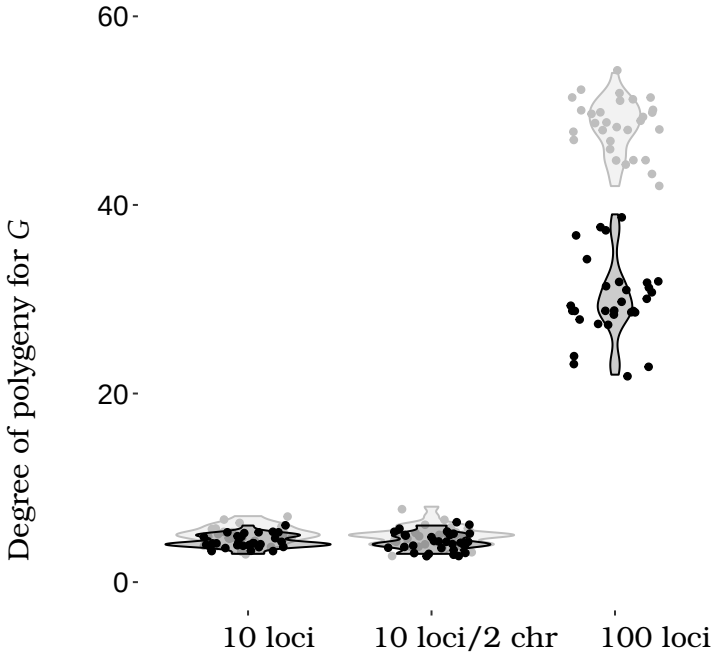

Figure B5: Degree of polygeny for the gametic investment. The measures are showed initially (in grey) and after evolution over 5000 time step (in black) for 30 replications for each genetic map (10 loci on 10 chromosomes, 10 loci on 2 chromosomes and 100 loci on 100 chromosomes). Greyed areas indicate density probability for the distribution of points in the variation range.

Appendix C: Electronic Enhancements

The model can be downloaded at `https://forgemia.inra.fr/louise.chevalier/runaway`to explore alternative scenarios.

Literature Cited

Bailey, N. W., Moore, A. J., 2012. Runaway sexual selection without genetic correlations: social environments and flexible mate choice initiate and enhance the fisher process. Evolution: International Journal of Organic Evolution 66 (9), 2674–2684.

Bengston, S. E., Dahan, R. A., Donaldson, Z., Phelps, S. M., Van Oers, K., Sih, A., Bell, A. M., 2018. Genomic tools for behavioural ecologists to understand repeatable individual differences in behaviour. Nature ecology & evolution 2 (6), 944–955.

Bolnick, D. I., Barrett, R. D., Oke, K. B., Rennison, D. J., Stuart, Y. E., 2018. (non) parallel evolution. Annual Review of Ecology, Evolution, and Systematics 49, 303–330.

Bonduriansky, R., Chenoweth, S. F., 2009. Intralocus sexual conflict. Trends in ecology & evolution 24 (5), 280–288.

Chapman, T., Arnqvist, G., Bangham, J., Rowe, L., 2003. Sexual conflict. Trends in Ecology & Evolution 18 (1), 41–47.

Charlesworth, D., Wright, S. I., 2001. Breeding systems and genome evolution. Current opinion in genetics & development 11 (6), 685–690.

Cheverud, J. M., 1996. Developmental Integration and the Evolution of Pleiotropy. Integrative and Comparative Biology 36 (1), 44–50.
URL http://icb.oxfordjournals.org/cgi/doi/10.1093/icb/36.1.44

Connallon, T., 2015. The geography of sex-specific selection, local adaptation, and sexual dimorphism. Evolution 69 (9), 2333–2344.

Darwin, C., 1872. The descent of man, and selection in relation to sex. Vol. 2. D. Appleton.

De Jong, M. C., Sabelis, M. W., 1991. Limits to runaway sexual selection: the wallflower paradox. Journal of Evolutionary Biology 4 (4), 637–655.

DeAngelis, D. L., Mooij, W. M., 2005. Individual-based modeling of ecological and evolutionary processes. Annu. Rev. Ecol. Evol. Syst. 36, 147–168.

Debarre, F., Otto, S. P., 2016. Evolutionary dynamics of a quantitative trait in a finite asexual population. Theoretical population biology 108, 75–88.

Dechaume-Moncharmont, F. X., Brom, T., Cézilly, F., 2016. Opportunity costs resulting from scramble competition within the choosy sex severely impair mate choosiness. Animal Behaviour 114 (April), 249–260.

Dufour-Kowalski, S., Courbaud, B., Dreyfus, P., Meredieu, C., De Coligny, F., 2012. Capsis: an open software framework and community for forest growth modelling. Annals of forest science 69 (2), 221–233.

Eyre-Walker, A., Keightley, P. D., 1999. High genomic deleterious mutation rates in hominids. Nature 397 (6717), 344–347.

Falconer, D. S., Mackay, T. F., Frankham, R., 1996. Introduction to quantitative genetics (4th edn). Trends in Genetics 12 (7), 280.

Fawcett, T. W., McNamara, J. M., Houston, A. I., Feb. 2012. When is it adaptive to be patient? a general framework for evaluating delayed rewards. Behavioural Processes 89 (2), 128–136.

Fisher, R., 1930. The genetical theory of natural selection oxford univ. Press (Clarendon), London (Reprinted and revised, 1958).

Fisher, R. A., 1915. The evolution of sexual preference. The Eugenics Review 7 (3), 184.

Fromhage, L., Jennions, M. D., 2016. Coevolution of parental investment and sexually selected traits drives sex-role divergence. Nature communications 7 (1), 1–11.

Gibson, J. R., Chippindale, A. K., Rice, W. R., 2002. The x chromosome is a hot spot for sexually antagonistic fitness variation. Proceedings of the Royal Society of London. Series B: Biological Sciences 269 (1490), 499–505.

Gimelfarb, A., 1988. Processes of pair formation leading to assortative mating in biological populations: encounter-mating model. The American naturalist 131 (6), 865–884.

Grimm, V., Berger, U., Bastiansen, F., Eliassen, S., Ginot, V., Giske, J., Goss-Custard, J., Grand, T., Heinz, S. K., Huse, G., et al., 2006. A standard protocol for describing individual-based and agent-based models. Ecological modelling 198 (1-2), 115–126.

Griswold, C. K., 2006. Pleiotropic mutation, modularity and evolvability. Evolution & development 8 (1), 81–93.

Guillaume, F., Otto, S. P., 2012. Gene functional trade-offs and the evolution of pleiotropy. Genetics 192 (4), 1389–1409.

Haldane, J. B., 1935. The rate of spontaneous mutation of a human gene. Journal of genetics 31 (3), 317.

Hall, D. W., Kirkpatrick, M., West, B., 2000. Runaway sexual selection when female preferences are directly selected. Evolution 54 (6), 1862–1869.

Hammer, M. F., Mendez, F. L., Cox, M. P., Woerner, A. E., Wall, J. D., 2008. Sex-biased evolutionary forces shape genomic patterns of human diversity. PLoS genetics 4 (9).

Hansen, T. F., 2003. Is modularity necessary for evolvability? Remarks on the relationship between pleiotropy and evolvability. BioSystems 69 (2-3), 83–94.

Hendry, A. P., Kinnison, M. T., 1999. Perspective: the pace of modern life: measuring rates of contemporary microevolution. Evolution 53 (6), 1637–1653.

Hill, W. G., Zhang, X.-S., 2012. On the pleiotropic structure of the genotype–phenotype map and the evolvability of complex organisms. Genetics 190 (3), 1131–1137.

Iwasa, Y., Pomiankowski, A., 1995. Continual change in mate preferences. Nature 377 (6548), 420.

Iwasa, Y., Pomiankowski, A., Nee, S., 1991. The Evolution of Costly Mate Preferences II. The 'Handicap' Principle. Evolution 45 (6), 1431.

Jones, A. G., Arnold, S. J., Bürger, R., 2003. Stability of the g-matrix in a population experiencing pleiotropic mutation, stabilizing selection, and genetic drift. Evolution 57 (8), 1747–1760.

Jones, A. G., Arnold, S. J., Bürger, R., 2007. The mutation matrix and the evolution of evolvability. Evolution 61 (4), 727–745.

Jones, A. G., Bürger, R., Arnold, S. J., 2014. Epistasis and natural selection shape the mutational architecture of complex traits. Nature communications 5 (1), 1–10.

Jones, A. G., Ratterman, N. L., 2009. Mate choice and sexual selection: what have we learned since darwin? Proceedings of the National Academy of Sciences 106 (Supplement 1), 10001–10008.

Kent, C., Azanchi, R., Smith, B., Formosa, A., Levine, J. D., 2008. Social context influences chemical communication in d. melanogaster males. Current Biology 18 (18), 1384–1389.

Kokko, H., Booksmythe, I., Jennions, M. D., 2015. Mate-sampling costs and sexy sons. Journal of evolutionary biology 28 (1), 259–266.

Kokko, H., Jennions, M. D., 2008. Parental investment, sexual selection and sex ratios. Journal of Evolutionary Biology 21 (4), 919–948.

Krupp, J. J., Kent, C., Billeter, J.-C., Azanchi, R., So, A. K.-C., Schonfeld, J. A., Smith, B. P., Lucas, C., Levine, J. D., 2008. Social experience modifies pheromone expression and mating behavior in male drosophila melanogaster. Current Biology 18 (18), 1373–1383.

Lamichhaney, S., Fan, G., Widemo, F., Gunnarsson, U., Thalmann, D. S., Hoeppner, M. P., Kerje, S., Gustafson, U., Shi, C., Zhang, H., et al., 2016. Structural genomic changes underlie alternative reproductive strategies in the ruff (philomachus pugnax). Nature Genetics 48 (1), 84–88.

Lande, R., 1976. Natural selection and random genetic drift in phenotypic evolution. Evolution 30 (2), 314–334.

Lande, R., 1980. The genetic covariance between characters maintained by pleiotropic mutations. Genetics 94 (1), 203–215.

Lande, R., 1981. Models of speciation by sexual selection on polygenic traits. Proceedings of the National Academy of Sciences 78 (6), 3721–3725.

Lande, R., Arnold, S. J., 1985. Evolution of mating preferences and sexual dimorphism. Journal of Theoretical Biology 117 (4), 651–664.

Lehtonen, J., Jennions, M. D., Kokko, H., 2012. The many costs of sex. Trends in ecology & evolution 27 (3), 172–178.

Lehtonen, J., Parker, G. A., Schärer, L., 2016. Why anisogamy drives ancestral sex roles. Evolution 70 (5), 1129–1135.

Lorch, P. D., Proulx, S., Rowe, L., Day, T., 2003. Condition-dependent sexual selection can accelerate adaptation. Evolutionary Ecology Research 5 (6), 867–881.

Matessi, C., Di Pasquale, C., 1996. Long-term evolution of multilocus traits. Journal of Mathematical Biology 34 (5-6), 613–653.

Matuszewski, S., Hermisson, J., Kopp, M., 2014. Fisher's geometric model with a moving optimum. Evolution 68 (9), 2571–2588.

Mead, L. S., Arnold, S. J., 2004. Quantitative genetic models of sexual selection. Trends in ecology & evolution 19 (5), 264–271.

Misevic, D., Ofria, C., Lenski, R. E., 2006. Sexual reproduction reshapes the genetic architecture of digital organisms. Proceedings of the Royal Society B: Biological Sciences 273 (1585), 457–464.

Moore, A. J., Brodie III, E. D., Wolf, J. B., 1997. Interacting phenotypes and the evolutionary process: I. direct and indirect genetic effects of social interactions. Evolution 51 (5), 1352–1362.

Muller, H. J., 1928. The measurement of gene mutation rate in drosophila, its high variability, and its dependence upon temperature. Genetics 13 (4), 279.

Muniz, D. G., Machado, G., 2018. Mate sampling influences the intensity of sexual selection and the evolution of costly sexual ornaments. Journal of theoretical biology 447, 74–83.

Oddou-Muratorio, S., Davi, H., 2014. Simulating local adaptation to climate of forest trees with a physio-demo-genetics model. Evolutionary applications 7 (4), 453–467.

Oke, K. B., Rolshausen, G., LeBlond, C., Hendry, A. P., 2017. How parallel is parallel evolution? a comparative analysis in fishes. The American Naturalist 190 (1), 1–16.

Otto, S. P., 2004. Two steps forward, one step back: the pleiotropic effects of favoured alleles. Proceedings of the Royal Society of London. Series B: Biological Sciences 271 (1540), 705–714.

Otto, S. P., Servedio, M. R., Nuismer, S. L., 2008. Frequency-dependent selection and the evolution of assortative mating. Genetics 179 (4), 2091–2112.

Paaby, A. B., Rockman, M. V., 2013. The many faces of pleiotropy. Trends in Genetics 29 (2), 66–73.

Parker, G. A., Baker, R. R., Smith, V. G. F., 1972. The origin and evolution of gamete dimorphism and the male-female phenomenon. Journal of Theoretical Biology 36 (3), 529–553.

Pigliucci, M., 2008. Is evolvability evolvable? Nature Reviews Genetics 9 (1), 75–82.

Piou, C., Prévost, E., 2012. A demo-genetic individual-based model for atlantic salmon

populations: Model structure, parameterization and sensitivity. Ecological Modelling 231, 37–52.

Plomion, C., Aury, J.-M., Amselem, J., Leroy, T., Murat, F., Duplessis, S., Faye, S., Francillonne, N., Labadie, K., Le Provost, G., et al., 2018. Oak genome reveals facets of long lifespan. Nature Plants 4 (7), 440–452.

Pomiankowski, A., Iwasa, Y., 1998. Runaway ornament diversity caused by fisherian sexual selection. Proceedings of the National Academy of Sciences 95 (9), 5106–5111.

Ramsey, D. M., 2011. Mutual mate choice with multiple criteria. In: Advances in dynamic games. Springer, pp. 337–355.

Ritchie, M. G., 2007. Sexual Selection and Speciation. Annual Review of Ecology, Evolution, and Systematics 38 (7), 79–102.

Rittschof, C. C., Robinson, G. E., 2014. Genomics: Moving behavioural ecology beyond the phenotypic gambit. Animal Behaviour 92, 263–270.

Roff, D., Mousseau, T., 1999. Does natural selection alter genetic architecture? an evaluation of quantitative genetic variation among populations of allenomobius socius and a. fasciatus. Journal of Evolutionary Biology 12 (2), 361–369.

Sasaki, A., Dieckmann, U., 2011. Oligomorphic dynamics for analyzing the quantitative genetics of adaptive speciation. Journal of mathematical biology 63 (4), 601–635.

Schwartz, A. K., Hendry, A. P., 2007. A test for the parallel co-evolution of male colour and female preference in trinidadian guppies (poecilia reticulata). Evolutionary Ecology Research 9 (1), 71–90.

Shaw, F. H., Shaw, R. G., Wilkinson, G. S., Turelli, M., 1995. Changes in genetic variances and covariances: G whiz! Evolution 49 (6), 1260–1267.

Sinervo, B., Svensson, E., 2002. Correlational selection and the evolution of genomic architecture. Heredity 89 (5), 329–338.

Smith, M., 1976. the theory of games: In situations characterized by conflict of interest, the best strategy to adopt depends on what others are doing. Am. Sci 64, 41–45.

Steppan, S. J., Phillips, P. C., Houle, D., 2002. Comparative quantitative genetics: evolution of the g matrix. Trends in Ecology & Evolution 17 (7), 320–327.

Tazzyman, S. J., Iwasa, Y., 2010. Sexual selection can increase the effect of random genetic drift—a quantitative genetic model of polymorphism in oophaga pumilio, the strawberry poison-dart frog. Evolution: International Journal of Organic Evolution 64 (6), 1719–1728.

Wakano, J. Y., Iwasa, Y., 2013. Evolutionary branching in a finite population: deterministic branching vs. stochastic branching. Genetics 193 (1), 229–241.

Wakano, J. Y., Lehmann, L., 2014. Evolutionary branching in deme-structured populations. Journal of theoretical biology 351, 83–95.

Walsh, B., Blows, M. W., 2009. Abundant Genetic Variation + Strong Selection = Multivariate Genetic Constraints: A Geometric View of Adaptation. Annual Review of Ecology, Evolution, and Systematics 40 (1), 41–59.

West-Eberhard, M. J., 1983. Sexual selection, social competition, and speciation. The Quarterly Review of Biology 58 (2), 155–183.

Wilbur, H. M., Rudolf, V. H., 2006. Life-history evolution in uncertain environments: bet hedging in time. The American Naturalist 168 (3), 398–411.

Wilkinson, G. S., Breden, F., Mank, J. E., Ritchie, M. G., Higginson, A. D., Radwan, J., Jaquiery, J., Salzburger, W., Arriero, E., Barribeau, S., et al., 2015. The locus of sexual selection: moving sexual selection studies into the post-genomics era. Journal of evolutionary biology 28 (4), 739–755.

Wolf, J. B., Brodie III, E. D., Moore, A. J., 1999. Interacting phenotypes and the evolutionary process. ii. selection resulting from social interactions. The American Naturalist 153 (3), 254–266.